Stability Evaluation of the 1 GeV Electron Beam by a Particle-dynamics Code

Takao ASAKA

SPring-8/JASRI

1. Introduction

In beam operations or measurement of beam qualities, it is important to stabilize the beam energy and energy spread of the 1 GeV injector linac. In order to realize uniformity of the bunch train in the storage ring, it has to satisfy the requirements of both the reproducibility and stability of beam energy at the injector linac, which has a lot of high power RF equipment. The energy stability as well as the beam transmission stability has been a very important issue for stable injection to the synchrotron ring since the operation of the synchrotron ring began in December 1996. It was observed that the drift of the beam current had a period of 25 minutes at the LSBT. In addition, the beam current varied gradually during the measurement of 10 hours [1].

In order to investigate the drift of the RF parameters related to the klystrons, which can be influenced by outside factors, the cooling water temperature and the environmental temperature were measured. It turns out that the phase of klystrons coincide with the cooling water temperature drift. Although controlled by an air conditioning, the room temperature can vary about 4.0˚C in the course of a day, affecting the high power klystron drive system. Furthermore, the shot-by-shot center-energy fluctuation was expected to be caused by PFN voltage fluctuation of the 13-set klystron modulator, along with the jitter of the modulator and thyratron triggers.

2. Beam Stability after Improvements

In order to reduce the long-term phase drift of the high-power klystron drive system [2], its 70 m waveguide was covered with a heat insulator. In addition, the priority of humidity control was replaced by the priority of room temperature control in the klystron gallery. After these improvements, the phase drift of the high power drive system was achieved at levels smaller than 3.0 deg. through one day as shown in Fig.1.

In the cooling water control for klystron cavities, the fan control of the coolant tower had been improved to continuous rotation by using an inverter control from a switching system like an on/off control. After this improvement, the phase stability of the klystrons were reduced within 0.5 deg. in steady state operation as shown in Fig.2.

As readjustment was made to the specified de-Qing efficiency value of 7.0 %, the PFN voltage stability achieved 0.1% (1σ) for each klystron. The reproducibility and stability of the beam status after the above improvements realized a beam current of 0.7 % (1σ) and a center energy of 0.1 % (1σ) at the LSBT in which a wall current monitor and a beam position monitor was installed as illustrated Fig. 3. Figure 4 shows the log data of the beam current and center energy at the LSBT.

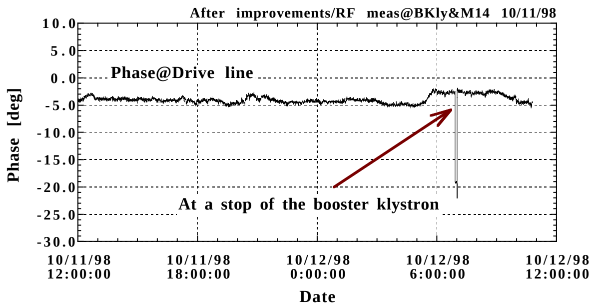

Fig. 1. Phase drift for the drive line at the M14 IϕA.

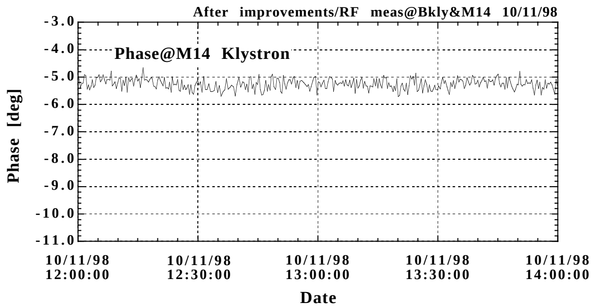

Fig. 2. Phase drift for the 80-MW klystron (M14).

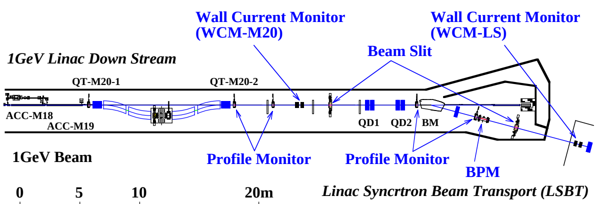

Fig. 3. Layout of linac- synchrotron beam transport.

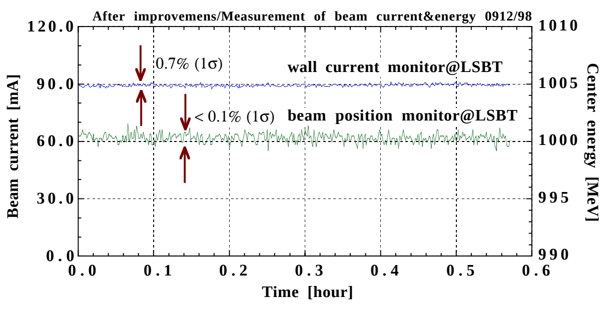

Fig. 4. Log data of beam current and center energy.

3. Stability of the Klystrons

3.1 80-MW Klystrons for Main Accelerating Section

The power and phase drift of klystron were affected not only by the cooling water temperature, which had a period of 25 minutes, but also by a random fluctuation of the PFN voltage at the 80 MW klystron pulse modulator. Although the PFN voltage of all of the pulse modulators had to be regulated with the stability of ± 0.5 % by the de-Qing system, the PFN voltage fluctuation of the M14 pulse modulator, for example was ±1.0 % due to the inadequate adjustment of the de-Qing efficiency. The PFN voltage stability of all the pulse modulators in continuous operation of 12 hours is given in Table 1.

For the voltage fluctuation δV_k of a pulse modulator, the power fluctuation δP_k and the phase fluctuation $\delta\theta_k$ of a klystron are

$$\delta P_k = \frac{5}{2}\,\alpha_{loss}\,\eta_k\,k\,V_k^{3/2}\,\delta V_k\,,$$

$$\delta\theta_k = -2\,\pi\,f\,l_k\,\frac{1}{c}\,\frac{e}{m_0\,c^2}\left\{\left(\frac{e\,V_k}{m_0\,c^2}+1\right)^2-1\right\}^{-\frac{3}{2}}\delta V_k\,,$$

where α_{loss}, η_k, k, V_k, l_k are the waveguide loss, the efficiency, the perveance, the cathode voltage and the distance from an input coupler to an output coupler of a klystron, respectively. The relation between the RF power P_k and the accelerating field E is expressed as

$$E = \sqrt{P_k\,R_s\,l_{acc}\left(1-\exp(-2\,\tau)\right)}\,,$$

where R_s, l_{acc} and τ are the shunt impedance, physical length and attenuation parameter of a structure. The energy variation δE_{total} resulting from δV_k is expressed as

$$\delta E_{total} = \left(E_{crest} + \delta E\right)\cos\left(\delta\theta_k\right)\,.$$

From the above equations, the total beam energy shift is calculated to be 0.2 % (1σ), which agrees with the result of the measurement value.

Table 1. PFN voltage stability of the pulse modulators (measurement time : 12 hours)

	Klystron beam voltage (mean) [kV]	Dispersion (1σ) [%] Before adjustment	Dispersion (1σ) [%] After adjustment
Booster	137.3	0.3	0.16
H0	310.4	1.1	0.25
H1	337.3	0.6	0.21
H3	334.1	0.8	0.22
H5	353.5	0.3	0.22
M2	-	-	-
M4	338.2	0.4	0.20
M6	351.8	0.4	0.21
M8	350.3	0.4	0.20
M10	-	-	-
M12	337.4	0.6	0.22
M14	325.6	1.0	0.22
M16	-	-	-
M18	364.1	0.6	0.19

3.2. 5-MW Klystron for Bunching Section at 60-MeV Pre-injector Section

The 60-MeV preinjector consists of a 200 kV thermionic gun, two prebunchers, a 13-cell standing wave type buncher, a 3-m long accelerating structure, focus magnets and ordinary beam monitors as illustrated in Fig.5. The extracted 1-nsec and 40-nsec beam from the gun is shrunk to 15psec (full width) by the two pre-buncher and the 1st cell of the 13-cell buncher. After bunching, bunches are accelerated up to 60-MeV by the 13-cell buncher and 3-m long accelerating structure. The output power of a 5-MW booster klystron is fed into the bunching section and the 80-MW klystron drive system which has a 70-m waveguide with directional couplers and feed the divided into the power attenuator/phase shifter units (IϕA) placed at each 80-MW klystron.

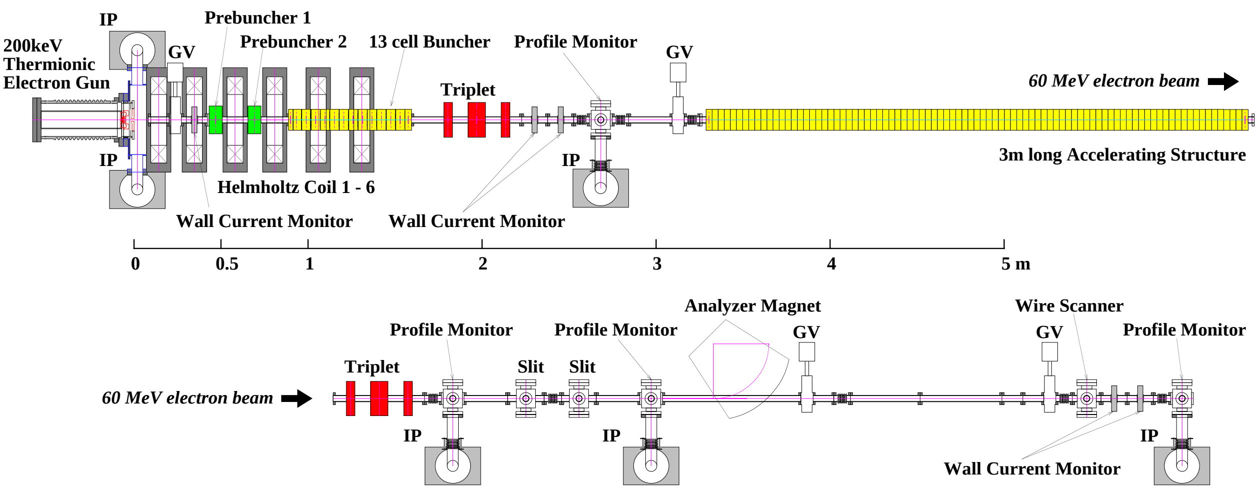

Fig. 5. Layout of the 60-MeV preinjector linac.

Since the velocity of electrons passing through the region from the gun to the 1st cell of buncher cavity is β = 0.7c, the bunching efficiency and acceleration process in the bunching section are sensitive to the RF power fluctuation of the 5-MW booster klystron. We found observed discrete variations of ± 0.2 % and ± 0.5 % with the RF power of the 5-MW booster klystron.

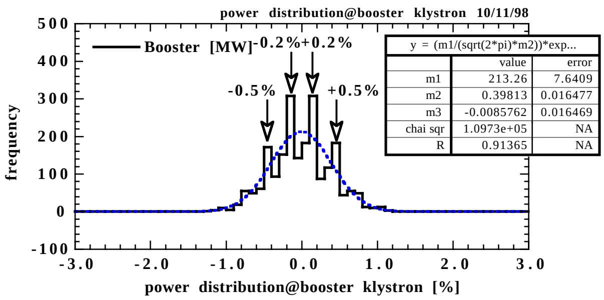

Fig. 6. RF power distribution of the 5-MW booster klystron for the bunching section.
(measurement time: 2 hours)

4. Simulation

Beam tracking simulations for the pre-injector were conducted using PARMELA, which calculates charged particle motion in 2.5 dimension. Input data for PARMELA refer the computed results from two codes: the beam characteristics of the gun were obtain by EGUN and the RF field in the cavity by SUPERFISH.

Figures 7.1, 7.2, 7.3 show examples of the beam bunch length and energy simulations, where we gave the RF power variation of ± 0.5 % at the bunching section. Figure 7.1 shows simulated beam parameters at the end of the 3-m accelerating structure where the beam energy is 65.843 MeV in case of the optimized magnetic and RF field parameters.

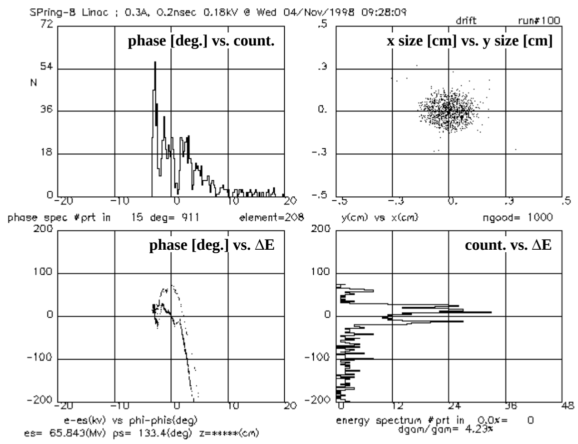

Fig. 7.1 The bunch length and energy distribution (65.843 MeV) at the end of the 1st accelerating structure with optimized parameters, upper-left) temporal distribution, upper-right) xy space, lower-left) longitudinal phase space, lower-right) energy distribution.

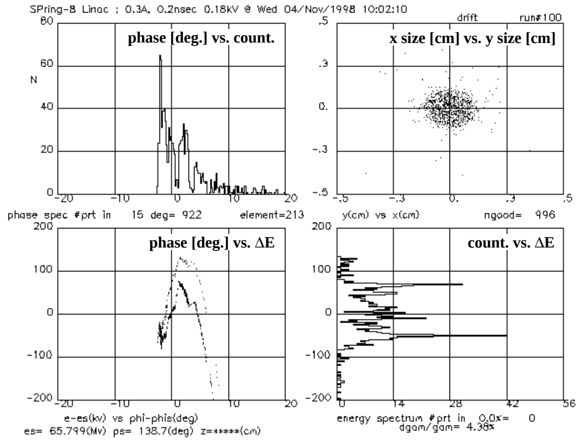

Fig. 7.2 The bunch length and energy distribution (65.799 MeV) at output of the 1st accelerating structure with the case of the RF power increase of + 0.5 % at the bunching section.

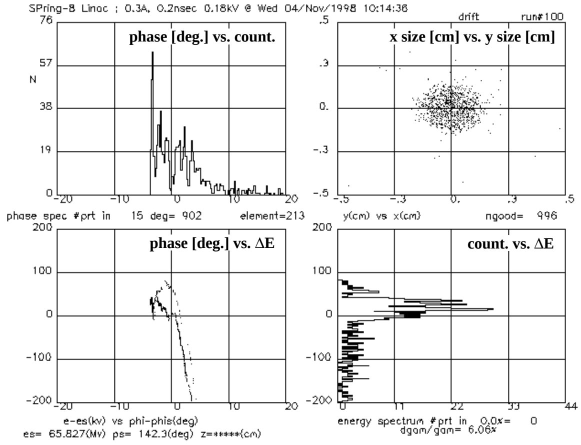

Fig. 7.3 The bunch length and energy distribution (65.827 MeV) at output of the 1st accelerating structure with the case of the RF power decrease of - 0.5 % at the bunching section.

The above results show that a beam energy shift of 0.1 % is cause by the power fluctuation of ± 0.5 % at bunching section. Furthermore, the energy spread increases in the case of the + 0.5 % power variation at the bunching section.

5. Summary

After improvements in the utility based on the measurement results of RF equipments, the stability of beam current at the LSBT could be maintained within 0.7% (1σ) in order to realize the energy stability of 0.1% (1σ). It turns out as a results of PARMELA simulation that the main accelerating section gives the energy fluctuation of 0.2% (1σ) and the preinjector gives 0.1% (1σ).

References

[1] T. Asaka et *al.*,"Stability of the RF system at the SPring-8 linac", Proc. of the 18th Particle Accelerator Conference, New York city, March 1999.

[2] S. Suzuki *et al.*, "Construction of SPring-8 Linac", Proc. of 4th European Accelerator Conf., London, July 1994.